



Deliverable D10.3

WP10 – JRA04 – INDESYS

**Detectors coating and compacting – Report on the progress achieved in the housing of hygroscopic scintillation materials with low interactive materials and minimal interacting passivating covers for Ge detectors**

The D10.3 report is presented in the following pages.

# Report on the development of the progress achieved in the housing of hygroscopic scintillation materials with low-interactive materials and minimal-interacting-passivating covers for Ge detectors

## 1) Housing of hygroscopic scintillation materials with low-interactive materials

### CsI(Tl) crystal wrapping

In order to capitalise on the CsI:Tl crystal properties it is essential that the light produced during scintillation is delivered without loss or degradation to the light sensor. In addition to the intrinsic crystal properties of the scintillator material, the wrapping surrounding the crystals is crucial. Firstly, it must have an unparalleled reflectivity, as any losses are directly represented in a degradation of the energy resolution. Secondly, it must be water-tight, as the CsI:Tl crystals have a degree of hygroscopicity which could lead to crystal erosion over time should the proper precautions not be taken. Thirdly, the material must not allow a non-negligible fraction of the internal light to be transmitted to neighbouring crystals, as this light cross-talk would contaminate the measurement. Finally, the material thickness and density must be minimised, as dead material will have a drastic effect on calorimetric ability for high multiplicity event reconstruction, in particular with regards to inter-crystal proton scattering. The importance of which is demonstrated in Fig 1, which shows the effect on proton energy resolution over a range of different wrapping thicknesses using the Montecarlo simulation package Geant4.

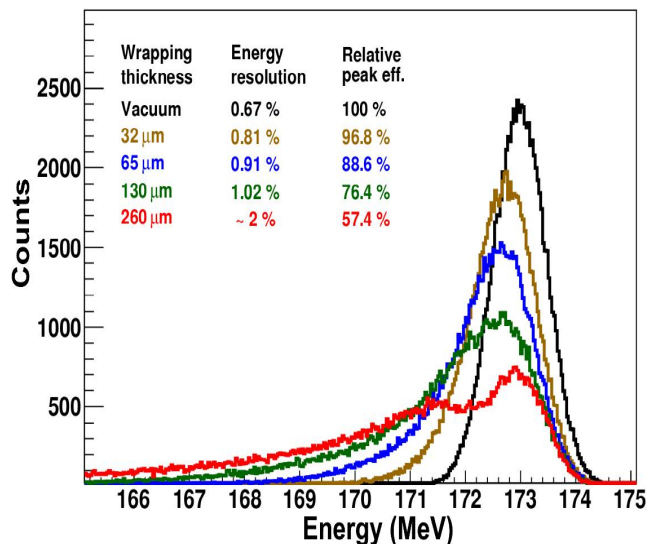


Fig 1: Simulations of the energy peak observed for 173~MeV incident protons using different thicknesses of crystal wrapping. Shown is for crystal multiplicity 2 events (see M. Gascón et al IEEE 55 (2008))

Following an intensive R&D campaign using several candidate materials, the wrapping ESR ( Enhanced Specular Reflector 3M) was selected, primarily for its excellent reflective qualities. The thickness used was 65  $\mu\text{m}$ , with a single wrapping encapsulating each crystal (see B. Pietras et al , NIM (2013)). A set of four wrapped crystals, with APDs attached, may be seen on Fig 2, below.

The light cross-talk was measured at the IFJ Pan, Bronowice cyclotron center (Cyclotron Center Bronowice, Poland), where proton energies ranging from 70 – 220 MeV were measured. The cross-talk between the crystals was measured to be an average of 1 %, as can be seen on Fig 3.



Fig 2: A set of four CsI crystals, wrapped in ESR, as would be held in a single carbon fibre alveolus. Mounted on the exit face are the accompanying Hamamatsu S12102 double APDs.

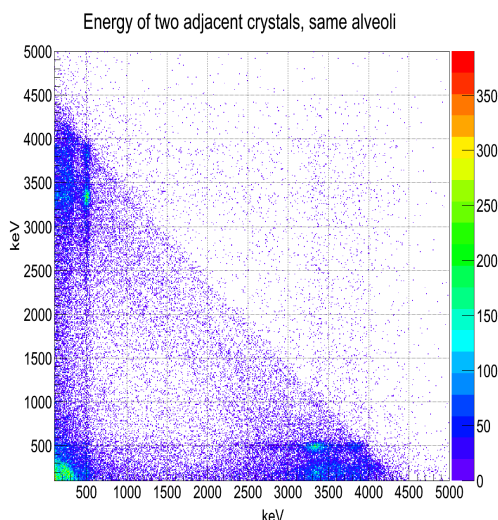


Fig 3: The respective energy spectrums of two single-layer ESR wrapped adjacent crystals measuring a  $^{244}\text{Cm}+^{13}\text{C}$  6.1~MeV source: the lack of light cross-talk may be clearly observed

## 2) Low-interactive materials and minimal-interacting-passivating covers for Ge detectors

The mature technology of perfect Ge crystal-growth, the donor/acceptor loading with precise doping levels, the extremely low reachable net-impurity level has been exploited since many decades for the fabrication of  $\gamma$ -rays detectors based on high purity Ge crystals (HPGe) with unsurpassed energy resolution with respect to scintillator detectors. For several years this niche of application has been almost the only one where germanium was considered as leading material. Recently, the increasingly demanding miniaturization of electronic devices reached the limit intrinsic to the physical nature of silicon and a renewed interest in SiGe and Ge-based MOS-based devices can be perceived, as shown by literature flourishing on this topic [<sup>i</sup>,<sup>ii</sup>]. Ge displays higher mobility of carriers and lower bandgap than silicon, holding the disadvantage of lack in surface

passivation. The  $\text{GeO}_x$  native oxide, composed of the unstable  $\text{GeO}$  and hydrosoluble  $\text{GeO}_2$  [iii, iv], does not compete with the high stability, ease of formation and thickness control of  $\text{SiO}_2$ .

In the specific field of  $\gamma$ -rays detectors, proprietary passivation layers are used, whose dielectric performance is excellent for charge collection from the full active volume of the detector, though recent studies reported that remarkably thick dead layers, where charge collection is hampered by distortions of the electric field [v], were found in commercial HPGe detectors [vi]. Thus, the research was oriented to passivation layers with low surface resistance to inhibit leakage currents, but at the same time not inducing thick dead layers. Many authors performed important work devoted to Ge surface treatments and to structural and electrical characterization of as-grown top layer; treatments studied include sulphidation [vii, viii, ix], controlled oxidation [x], and atomic layer deposition [xi]. Nevertheless, it is still an open topic the application of surface passivation to improve the performance of HPGe detectors, as related to leakage currents reduction and energy resolution enhancement. In comparison with evaluation of electrical performances of Ge-based devices for microelectronics, this argument has scarcely been explored.

In this work, the results of different wet chemical treatments for the surface passivation of an HPGe  $\gamma$ -rays detector are reported, giving particular attention to surface chemical interactions with top Ge atoms and consequent modifications of the I-V characteristics of the diode itself. The structural evolution of top surface layers with focus on the originated chemical bonds is investigated by IR spectroscopy in horizontal attenuated total reflectance mode (HATR) and by X-Ray Photoelectron Spectroscopy (XPS). The features of the newly generated bonds have been tested by the electrical response of a working HPGe diode, in order to check the effectiveness of the applied chemical treatment to block charge carriers loss across the inter-electrodes surface of the diode. Moreover, aging tests for stability evaluation are carried out by exposing the samples to ambient air for one month.

## Experimental

Ge <100> wafers, 2" in diameter and 500  $\mu\text{m}$  thick, were purchased from Umicore Ltd (Belgium, Olen) and preliminary polished by manual lapping with a slurry of bidistilled water (BDW) and alumina abrasive grains, with decreasing grain size from 30  $\mu\text{m}$  to 3  $\mu\text{m}$ . After each polishing step, the wafer was washed in ultrasonic bath with BDW to allow complete removal of alumina grains. The clean, mirror-like wafer was cut in small slabs, about 15x15 mm, washed in BDW and ultrasonic bath, rinsed several times in BDW, acetone and isopropanol. These Ge samples were used for XPS measurements; while for ATR-IR measurements the Ge crystal plate (entry face 45°, 20 reflections) used as dispersing elements in horizontal ATR method was used (Pike Technologies). For electrical measurements, an *n*-type HPGe diode, with planar geometry (thickness 21 mm, diameter 39 mm) was used (fabricated at the Laboratori Nazionali di Legnaro).

Chemicals (Carlo Erba Reagents, analytical grade) used for treatments were hydrogen peroxide  $\text{H}_2\text{O}_2$  at 30% hydrofluoric acid HF at 39.5% (or 50.0%), nitric acid  $\text{HNO}_3$  at 65%, ammonium sulphide  $(\text{NH}_4)_2\text{S}$  at 20% and methyl alcohol  $\text{CH}_3\text{OH}$ . A brief summary of the adopted treatments and methods is reported in Table I.

For HATR measurements, the spectrum of the Ge crystal plate immersed in  $\text{H}_2\text{O}_2$  30% for 2 min, rinsed thoroughly in BDW, then dried with  $\text{N}_2$  is used as background and reference.

The reference sample for XPS was prepared by immersion in HF 10% for 2 min, rinsed in BDW and dried with N<sub>2</sub> blow (label: Ge\_ref).

The treatment commonly adopted as a first step in the fabrication of HPGe  $\gamma$ -rays detectors was applied as follows: (i) etching in mixture of HF:HNO<sub>3</sub> 3:1 (volume ratio) for 3 min, (ii) etch quenching with excess BDW, (iii) final rinse in BDW and N<sub>2</sub> drying (Ge\_QW). The approach used by Gurov [xii] for treatment of HPGe detectors was also carried out by repeating the same etching in HF/HNO<sub>3</sub> but using methanol for quenching instead of BDW; the sample was blown with dry nitrogen (Ge\_QM). The procedure for sulphur passivation was similar to previously reported ones [xiii, xiv, xv, xvi]: the crystal was etched in HF 2% for 5 min, rinsed twice in BDW and immediately transferred in hot (NH<sub>4</sub>)<sub>2</sub>S solution for 20 min at 60°C; then it was rinsed three times in BDW and blown with N<sub>2</sub> (Ge\_S). For the H termination, two procedures were adopted [xvii, xviii, xix]: the crystal was etched in HF 10% for 2 min and then rinsed in BDW. This operation was repeated five times; afterwards the crystal was blown with dry nitrogen, leading to low H termination (Ge\_H10). The second procedure, called high H termination (Ge\_H50), consisted in a single etching in HF 50% for 5 min, followed by thorough rinse in BDW and blowing. These two approaches were used to investigate their effectiveness in originating surface Ge-H bonds; indeed previous papers point to partial native oxide removal after HF treatment, irrespectively of the concentration, treatment time or number of repeated cycles [viii, xiv, xx].

Table I. Summary of applied chemical treatments.

Label	Chemicals	Notes
Ge_ref	HF 10% (diluted)	2 min
Ge_QW	Etching 3:1 (vol) with HNO <sub>3</sub> (65%):HF (39.5%)	3 min etching time, quenching in BDW
Ge_QM	Etching 3:1 (vol) with HNO <sub>3</sub> (65%):HF (39.5%)	3 min etching time, quenching in CH <sub>3</sub> OH
Ge_H10	HF 10% (diluted), BDW, 5 cycles	2 min dip time in HF
Ge_H50	HF 50% (concentrated)	5 min
Ge_S	HF 2%, (NH <sub>4</sub> ) <sub>2</sub> S 60°C	2 min dip in HF, 20 min in (NH <sub>4</sub> ) <sub>2</sub> S

FTIR measurements were performed using the spectrometer Jasco 660-plus, equipped with horizontal ATR (HATR) accessory (PIKE technology). The spectra were recorded with 4 cm<sup>-1</sup> of resolution.

Photoelectron spectroscopy measurements were performed using an Al K $\alpha$  unmonochromatized source (1486.7 eV) at a base pressure of 10<sup>-9</sup> Torr. The photoelectrons were analysed by a cylindrical hemispherical analyser (CHA) operating at a pass energy of 58 eV or lower.

For the electrical measurements the HPGe diode was put in a cryostat after each chemical passivation treatment, pumped down to a pressure lower 10<sup>-3</sup> Pa, cooled down to the liquid nitrogen temperature and its p-n junction properties were tested by reverse-

biasing the diode at increasing voltage up to 1100 V and measuring the reverse leakage current. The main contribution to the leakage current came from surface currents as related to the different chemical treatments, while the bulk contribution was negligible. The measurements were carried out by means of a Keithley 237 source-measurement unit, which can measure dc currents as low as 0.01 pA. In order to minimize the effects of parasitic currents and capacities on the measured current, triaxial cables were used to connect the unit to the diode.

## Results and Discussion

### Infrared analyses

In Fig. 1 the spectra of the Ge crystal after immersion in HF 10% (Ge\_H10) and 50% (Ge\_H50) for different times are shown. The components with negative absorption at about  $3250\text{ cm}^{-1}$  and  $1480\text{ cm}^{-1}$  can be ascribed to the removal of Ge-OH hydroxyl groups, which are formed during hydrogen peroxide immersion, according to literature data [xxi,xxii]. Other oxidation products are not detected:  $\text{GeO}_2$  is highly soluble in water and dissolves as soon as it is produced. The more stable GeO, which should be observed at about  $770\text{ cm}^{-1}$  [xxiii,xxiv], is not visible, probably because of the low detector sensitivity at this particular range of wavenumbers. Other components due to surface adsorbed water are visible as negative absorption at  $3500\text{ cm}^{-1}$  and  $1650\text{ cm}^{-1}$ .

Fig. 1. HATR-IR spectra collected from Ge crystal treated with HF 10% (Ge\_H10) and 50% (Ge\_H50) for different times. Data are stacked on the vertical axis.

The sharp peak at about  $2015\text{ cm}^{-1}$  indicates the formation of germanium hydride [xx] and its intensity increases with treatment times up to 3 min; the longer 5 min treatment does not induce further increase, suggesting that hydride termination reaches a plateau. Diluted hydrofluoric acid (10%) does not apparently induce appreciable surface changes, even for repeated HF/ $\text{H}_2\text{O}$  immersions, thus indicating incomplete surface coverage of the Ge crystal, as already reported in previous work [xiv], or difficult removal of Ge-OH bonds formed during immersion in  $\text{H}_2\text{O}_2$  and of native GeO oxide, which hinder hydride surface modification. Interestingly, when the crystal is immersed in the HF 50% bath, after about 2 min it starts to change in colour and it assumes a dark reddish appearance. As soon as it is plunged into BDW for rinsing, the red shade vanishes and the classic lustre, silvery glance reappears. In literature there is no evident trace of this red compound, but the intensive nature of the treatment and previous literature on HF etching of Ge points to the formation of a transient oxyfluoride germanate [xxv,xxvi], that should be readily dissolved during the treatment but can remain as adsorbate species in case of absence of stirring, as in the present treatment.

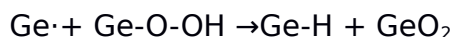
Spectra of Ge crystal after etching in  $\text{HNO}_3/\text{HF}$  3:1 mixture and quenched in BDW (Ge\_QW) or  $\text{CH}_3\text{OH}$  (Ge\_QM) are shown in Fig. 2. The signal of Ge-H is evident in both spectra at  $2010\text{-}2015\text{ cm}^{-1}$ . It must be noticed that the low signal/noise ratio in other spectral regions hampers the observation of possible signals due to Ge-O,  $\text{Ge-OCH}_3$  or Ge-OH. As a matter of fact, though etching time has been purposely kept as short as possible

(only 15 sec), the crystal size and shape are significantly modified by the etching treatment, which removes about 20  $\mu\text{m}/\text{min}$  in this concentration ratio [<sup>xxvii</sup>]. Hence, possible detrimental effects on the spectrum features are induced by not perfect background subtraction. In the case of methanol quenching, previous results reported by Bae and co-workers [<sup>xxviii</sup>] demonstrated the occurrence of dissociative adsorption of methanol as a result of exposure of clean Ge surface bearing highly reactive dangling bonds to methanol vapours; this fact may justify the weak component from Ge-H bonds. Though our method does not rely on vacuum annealed clean Ge surface, the freshly etched surface atoms are expected to have high chemical reactivity so that the mechanism proposed by Bae may likely be extended to our case.

Unexpectedly, in case of BDW quenching, Ge-H bonds are clearly detected, in spite of low peak intensity due to background subtraction. Indeed, only Ge-OH and Ge-O species resulting from hydroxylation or simple oxidation of surface Ge atoms are expected. A possible interpretation arises from the pioneering work of Harvey and Gatos on the reaction of germanium with aqueous solutions [<sup>xxix</sup>]. They considered water dissolved oxygen as electron acceptor, thus behaving as follows:



The -O-OH moiety represents the surface  $\equiv\text{Ge-O-OH}$  intermediate which can evolve to soluble metagermanic acid. The presence of vicinal Ge radicals may concurrently lead to hydride and hydrosoluble  $\text{GeO}_2$  through the reaction:



More recently, Steinert and co-workers [<sup>xxx</sup>] studied in detail the mechanism of silicon dissolution in  $\text{HNO}_3$  rich  $\text{HF}/\text{HNO}_3$  mixtures, as the one used in the present case, and using XPS analyses they revealed a surface termination with Si-H bonds, without Si-O nor Si-F bonds. This behaviour is explained in terms of divalent electrochemical dissolution, where nitric acid injects holes on the silicon surface atoms (oxidant action) thus making it susceptible of nucleophilic attack from HF or  $\text{HF}_2^-$  species. Consequently, a persistent hydride termination is present on silicon surface and hydrogen is released as reduction product. The proposed mechanism may apply also to the case of germanium etching in nitric/hydrofluoric acids mixtures, though remarkable differences in the etching behaviour of the two elements are known since a long time [<sup>xxv</sup>].

The spectrum (not reported) of the sample treated with ammonium sulphide Ge<sub>S</sub> does not show specific features.

Fig. 2. HATR-IR spectra of samples Ge<sub>QW</sub> and Ge<sub>QM</sub>.

XPS measurements

The Ge(2p) region of the XPS spectrum is more surface sensitive than Ge(3d) band owing to the smaller mean free path pertaining to Ge(2p) core level photoelectrons. Hence, possible changes in oxidation states of Ge top atoms should be better evidenced by the Ge(2p) band structure evolution. In the reference sample, Ge\_ref, the Ge 2p peak is at 1217.2 eV, in good agreement with previous assignments [xiv, xxiv, <sup>xxx</sup>]. However, the peak cannot be fitted with a single contribution and a second, weaker component, which can be ascribed to GeO, is found at 1218.6 eV [xx,xxxi]. Also in the Ge\_H10, Ge\_QW and Ge\_QM samples two components are present, as shown in Fig. 3, where the Ge 2p regions are reported, with relevant peaks deconvolution. The presence of GeO suboxide, even after repeated cycles of HF/H<sub>2</sub>O, was detected by several authors and discussed by Bodlaki [xiv]; clean Ge surfaces for subsequent thin films deposition or epitaxial growth require UHV flash annealing of the Ge wafer at temperatures as high as 1000 K [iv]. The relative amount of this residual suboxide or, conversely, the surface coverage with Ge-H bonds evaluated by different authors are not in agreement, in spite of applying the same procedure to remove the native oxide layer. This fact was attributed to different grades in the used reactants, either semiconductor grade or analytical grade, and also traced back to the brief lapse of time between the exposure to ambient air and the insertion in the analysis chamber, though much care has been devoted to blow inert gas over the sample during this operation.

As for the relative amount of GeO with respect to elemental Ge, it can be observed that for samples Ge\_ref (data not reported) and Ge\_QM the ratio between the integrals of the two components Ge:GeO is quite similar (about 7). This ratio further increases up to 8.4 in the sample Ge\_H10, thus evidencing a higher efficiency in the suboxide removal, resulting from repeated cycles HF/H<sub>2</sub>O, proposed by Deegan [xix], instead of a single dip in HF as done in the case of Ge\_ref.

A different behaviour is found for the sample Ge\_QW, which displays a much higher amount of the component ascribed to GeO or GeOH species, as shown by the remarkable Ge:GeO ratio reduction down to 2.6. In this case, the etching mechanism proposed for discussing the FTIR results may be recalled: the atop Ge surface, as-etched, is abruptly exposed to flushing water, thus promoting the partial saturation of surface radical sites by hydroxyl groups or bridging oxygen, though also Ge-H surface bonds are present as revealed by FTIR measurements. In the case of methanol quenching, the reactive surface promotes dissociative adsorption, as previously proposed [xxviii], leading to Ge-H and Ge-O-CH<sub>3</sub> covalent linkages, which provide effective shielding against oxidation, according to the low content of GeO shown by XPS measurements in the sample Ge\_QM (Ge:GeO ratio about 7).

The assignment of the component at higher binding energies is more difficult for the sample Ge\_S and a superposition of signals from residual oxide, GeO, and GeS<sub>2</sub>, resulting from sulphur bridging groups, can be envisaged. Maeda and co-workers [<sup>xxxii</sup>] proposed that saturation of surface sites of Ge(100) is achieved by coverage of one sulphur atom per surface Ge atom - GeS component at about +0.66 eV - and by two sulphur atoms per Ge - GeS<sub>2</sub> component at about +1.33 eV. The -S termination is confirmed by the appearance of S 2p peak (inset of Fig. 3) with a single spin-orbit doublet with energy separation of 1.2 eV [xiii,xxxii].

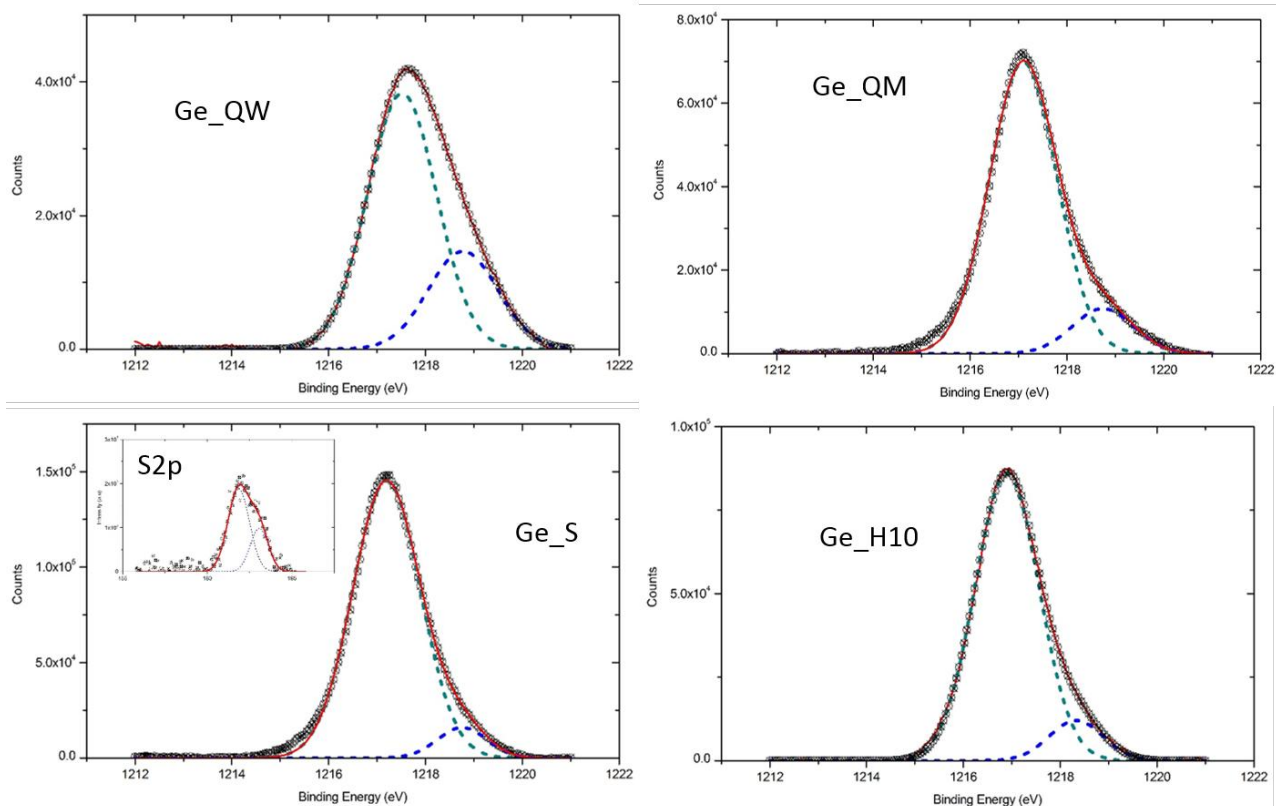


Fig. 3. XPS spectra of Ge<sub>2p</sub> peak, with corresponding peak deconvolution, for different wet treatments of the Ge surface.

Some interesting observations can be derived from C<sub>1s</sub> spectra reported in Fig. 4, which can provide indirect confirmation of previous description of differently passivated surfaces. The sample Ge<sub>ref</sub> displays the more intense carbon peak, as it was expected on the basis of the absence of any applied degreasing procedure and of the relatively weak treatment in diluted HF, so that the presence of adventitious carbon is relevant. However, the repeated cycles of HF/H<sub>2</sub>O applied for the preparation of Ge<sub>H10</sub> sample do not seem to be effective in complete removal of carbonaceous species, as proved by the still intense C<sub>1s</sub> signal. On one hand, this behaviour is in agreement with the results of Rivillon and co-workers [xx], who ascribe this contribution to the higher hydrophobicity and, in turn, higher affinity towards adventitious hydrocarbons of the H-terminated surface. On the other hand, very recently Seo and co-workers cast doubts on this interpretation [xxxiii] and it is suggested that the surface carbon species are so tightly bound to Ge atop atoms that the repeated dip cycles in HF are not enough to fully remove carbon contamination. On the basis of Auger spectroscopy data, Seo claims that the treatment of Ge in solution of ammonium hydroxide (NH<sub>4</sub>OH) can indeed drastically reduce carbon contamination owing to best solubility of the reaction by-products induced by complexation with ammonia. This reasoning can indeed be supported by our XPS data collected on Ge<sub>S</sub> sample, which displays the lowest content of surface carbon, indicating a possible contribution to effective Ge cleaning due to the presence of traces of ammonium hydroxide in equilibrium with un-buffered ammonium sulphide during the Ge<sub>S</sub> sample preparation. Moreover, the highly polar nature of the newly formed Ge-S bond (dipole moment is as high as 1.3 Debye vs 0.2 Debye of Ge-H bond [vii]) accounts

for the lower affinity towards almost apolar carbonaceous species, so that post-contamination with carbonaceous species is inhibited. Carbon is still present in the case of Ge\_QM, where surface grafting of Ge-OCH<sub>3</sub> methoxy groups can account for C presence, besides residual contamination from ambient air. The case of Ge-QW, where about the same carbon content is found, is more difficult to interpret. However, the possibility that the as-etched surface, bearing reactive Ge radicals, can react with CO<sub>2</sub> dissolved in water or that GeO/Ge-OH terminal groups undergo carbonation from reaction with CO<sub>2</sub> in ambient air cannot be ruled out. It is also worth to remember that FTIR revealed the presence of Ge-H bonds, which have high affinity with carbonaceous species.

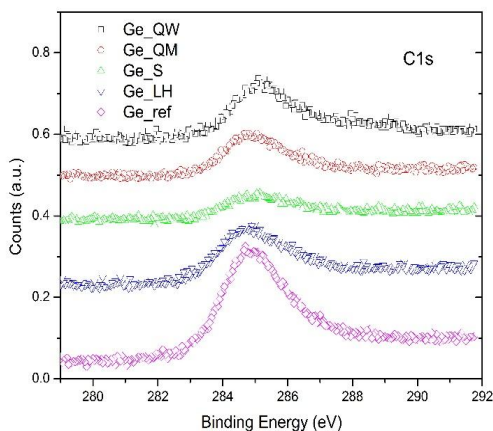


Fig. 4. XPS spectra of C1s region for different wet treatments of the Ge surface.

#### Ambient air stability: XPS study

The Ge2p spectra of samples collected after 1 month of ambient air exposure (relative humidity about 55 %) are shown in Fig. 5. It can be observed the growth of a quite intense component at +2.5-3.0 eV. This feature can be ascribed to GeO<sub>2</sub> layer formation, in agreement with previously reported data [xiv,xxiii,xxiv,xxxi]; air exposure firstly gives GeO<sub>x</sub> mixed oxides, but after few hours the structure GeO<sub>2</sub> becomes dominant. The GeO<sub>2</sub>/Ge ratio is about 1.8 for the reference sample Ge\_ref - single HF dip - while for repeated cycles the value is about 2.0 (sample Ge\_H10). In the sample Ge\_QW, where water was used to quench, the ratio is the highest one and reaches 4.1, leading to the conclusion that the presence of GeO/Ge-OH surface sites is less effective in hampering further oxidation than Ge-H bonds, though a limited amount of H-terminations has been revealed by FTIR analyses.

Quenching in methanol (sample Ge\_QM) appears as more “oxidation-proof”, since the ratio decreases to 3.7. In case of dissociative adsorption of methanol, the presence on the surface of low polar and hydrophobic Ge methoxide, with methyl external groups, and Ge-H bonds, which can contribute to oxidation resistance in humid air, as evidenced by the low contribution of GeO<sub>2</sub> in the sample Ge\_H10, accounts for this behaviour.

The most interesting result concerns the Ge\_S sample, which displays the lowest ratio between dioxide and elemental germanium ( $\text{GeO}_2/\text{Ge}$  about 1.3). This could be expected on the basis of the results of Lee and co-workers [xxiv], who explained the stronger stability of S-terminated Ge surface, as compared to H-termination, on the basis of several factors, such as bonding of S with two Ge surface atoms in a (2x1) structure, or formation of a glassy layer of  $\text{GeS}_x$ . Moreover, recalling the discussion above on the presence of residual adventitious carbon, it can be inferred that a greater surface coverage is achieved in the case of Ge\_S sample, owing to the almost complete removal of contamination carbon in alkaline medium, which leads to the maximum exposed area of Ge surface sites towards the sulphide reactant. Therefore, a better shielding against oxidation can be offered by the almost continuous layer of Ge-S surface bonds.

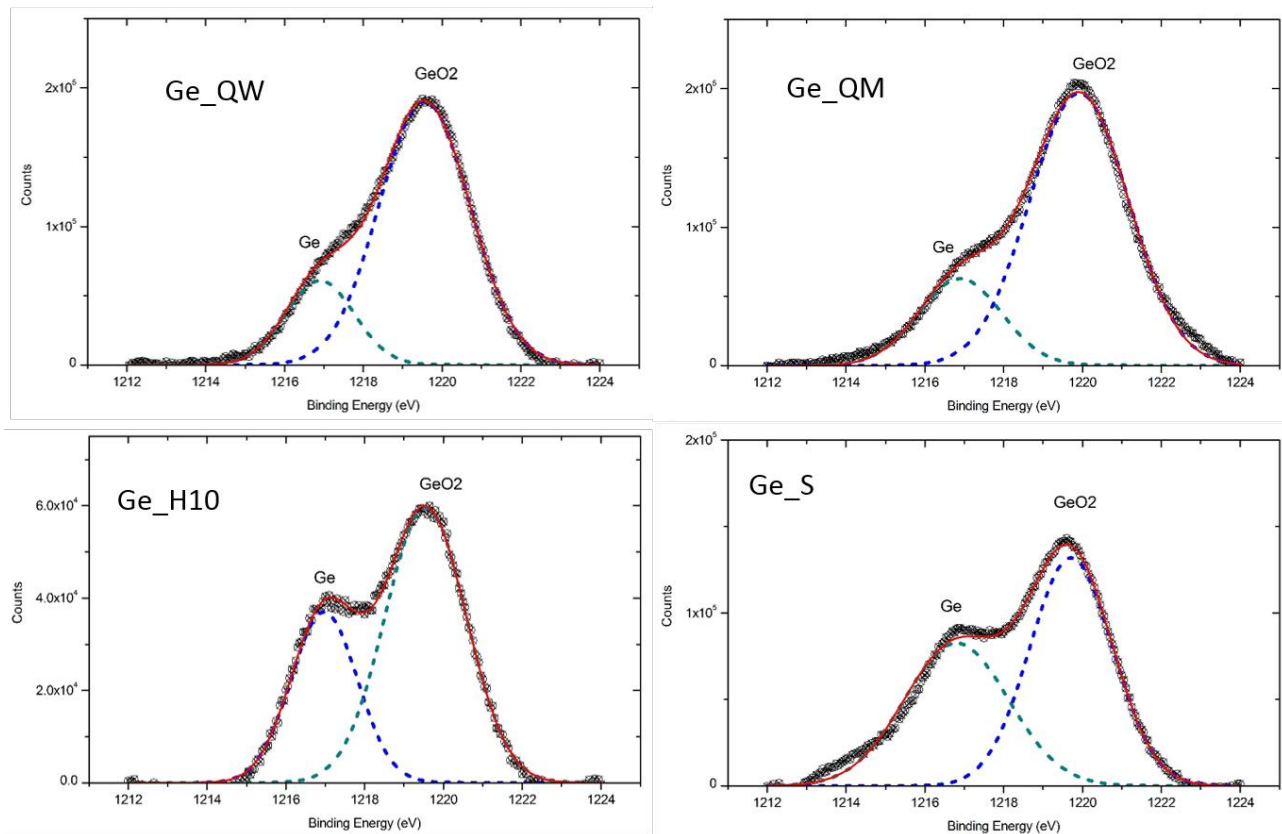


Fig. 5. Ge 2p core-level photoemission spectra with peak deconvolution for each chemical treatment, collected after 1 month of air exposure (RH about 55%).

### I-V measurements on HPGe diode

In order to test the effectiveness of the surface passivation by the chemical treatments studied in this work, the reverse leakage current of a planar HPGe diode was measured after each passivation. The resulting I-V data, as obtained by biasing the diode until a maximum applied voltage of 1100 V, are reported in Fig. 6. It can be observed that the reverse leakage current keeps very low in the whole measurement range, even at the highest applied voltage: at 1100 V the current is below 10 pA, for all the chemical treatments. This is an important premise for the application of these treatments as passivation routes of HPGe detectors, wherein a low leakage current is particularly

important to assure a good energy resolution in the detection of gamma radiation. These measurements also show that the breakdown voltage of the HPGe diode is well above 1100 V for all the tested passivations, thus assuring the complete charge depletion of the diode volume, necessary for using it as a totally-depleted detector [Knoll].

A more careful look at the curves in Figure 6 allows to find some small differences between them: at low voltage, the current of the Ge\_H50 diode is higher than that of the other passivations, while for the Ge\_H10 diode a slightly steeper increase is found in the high voltage region. On the other hand, the diode treated as in Ge\_S and Ge\_QM shows optimal performance over the entire range, with negligible fluctuations and with a leakage current lower than 4.5 pA. The S-terminated diode was also exposed to ambient air for 30 h (temperature 22°C, RH 66%) to test the stability of this passivation and the leakage current was measured again. Negligible changes were observed, thus confirming the durability of this passivation on this time scale [xiv]. These evidences are clues of the different electrical properties of the passivated surfaces, which affect the performance of the diode when used as  $\gamma$ -rays detector, especially energy resolution, efficiency, working voltage and dead layer thickness. The measurement campaign of this detector is still ongoing and the results will be published in a forthcoming paper [xxxiv].

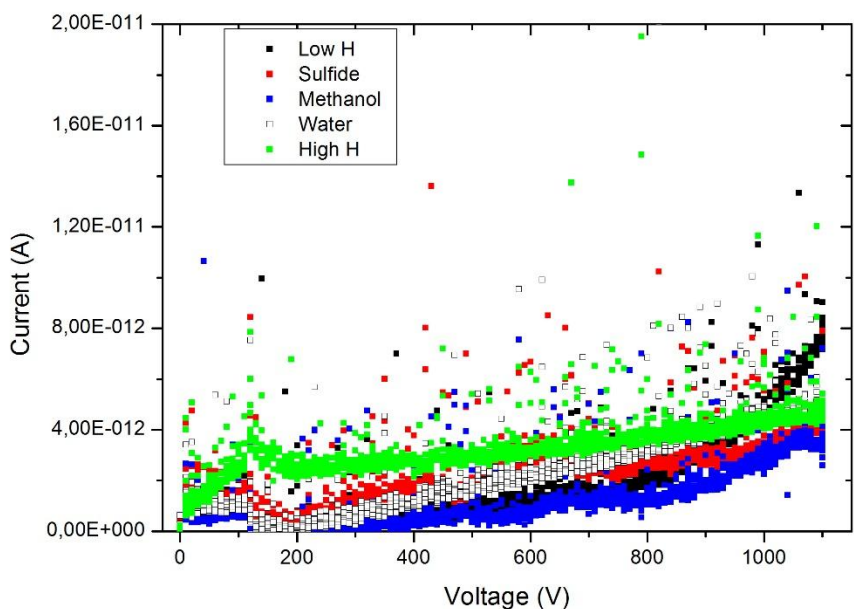


Fig. 6. I-V measurements obtained with HPGe diode after application of different passivation treatments.

## Conclusions

Different wet chemical passivation methods have been applied to either Ge small samples or HPGe working diode, aiming at the evaluation of effectiveness in minimizing leakage currents and charge carriers loss during HPGe working as  $\gamma$ -rays detector. HATR analysis has been performed to investigate the formation of Ge-H chemical bonds, in case

of treatment of freshly cleaned Ge shards in diluted and concentrated hydrofluoric acid. The appearance of Ge-H typical stretching mode occurs in case of dip in concentrated HF, demonstrating that the presence of mixed oxides, GeO and GeO<sub>2</sub>, on the native surface can hamper full coverage with H-terminated sites. Treatment of a freshly etched Ge surface with methanol also leads to the appearance of Ge-H band, indicating that dissociative mechanism of the methanol molecule takes place as soon as CH<sub>3</sub>OH reacts with highly reactive Ge surface radicals. XPS analyses confirm the results pointed out by HATR as regarding H-terminated Ge surface, and also allows to appreciate the effectiveness of S-termination and to follow the evolution in Ge surface changes as resulting from exposure to ambient air. Terminations with hydride and sulphide display the best oxidation resistance, suggesting successful inhibition of inter-electrodes leakage currents, which are detrimental for energy resolution of HPGe detector. Our surface treatments show optimal performances as passivating layers, as demonstrated by the ultra-low currents detected after application of voltage as high as 1100V; this fact may enhance the performance of HPGe  $\gamma$ -rays detectors, as foreseen by preliminary tests ongoing at the LNL laboratories.

## References

- [i] B. Colombeau, B. Guo, H.J. Gossmann, F. Khaja, N. Pradhan, A. Waite, K.V. Rao, C. Thomidis, K.H. Shim, T. Henry, N. Variam, *Phys. Status Solidi A*, 211 (2014) 101-108.
- [ii] Q. Xie, S. Deng, M. Schaekers, D. Lin, M. Caymax, A. Delabie, X.P. Qu, Y.L. Jiang, D. Deduytsche, C. Detavernier, *Semicond. Sci. Techn.* 27 (2012) 074012.
- [iii] K. Prabhakaran, T. Ogino, *Surf. Sci.* 325 (1995) 263-271.
- [iv] J.S. Hovis, R.J. Hamers, C.M. Greenlief, *Surf. Sci.* 440 (1999) L815-L819.
- [v] H. Utsunomiya, H. Akimune, K. Osaka, T. Kaihori, K. Furutaka, H. Harada, *Nucl. Instrum. Meth. A* 548 (2005) 455-463.
- [vi] J. Eberth, J. Simpson, *Progr. Particle Nucl. Phys.* 60 (2008) 283-337.
- [vii] C. Fleischmann, K. Schouteden, M. Müller, P. Hönicke, B. Beckhoff, S. Sioncke, H.-G. Boyen, M. Meuris, C. Van Haesendonck, K. Temsta, A. Vantomme, *J. Mater. Chem. C* 1 (2013) 4105.
- [viii] C. Fleischmann, S. Sioncke, S. Couet, K. Schouteden, B. Beckhoff, M. Müller, P. Hönicke, M. Kolbe, C. Van Haesendonck, M. Meuris, K. Temst, A. Vantomme, *J. Electrochem. Soc.* 158 (2011) H589-H594.
- [ix] K. Kasahara, S. Yamada, T. Sakurai, K. Sawano, H. Nohira, M. Miyao, K. Hamaya, *Appl. Phys. Lett.* 104 (2014) 172109.
- [x] A. Delabie, F. Bellenger, M. Houssa, T. Conard, S. Van Elshocht, M. Caymax, M. Heyns, M. Meuris, *Appl. Phys. Lett.* 91 (2007) art. no. 082904.
- [xi] Q. Xie, S. Deng, M. Schaekers, *Semicond. Sci. Techn.* 27 (2012) art. nr. 074012.
- [xii] Yu. B. Gurov, V.S. Karpukhin, S.V. Rozov, V.G. Sandukovsky, D. Borowicz, J. Kwiatkowska, B. Rajchel, J. Yurkowski, *Instrum. Experim. Techn.* 52 (2009) 137-140.
- [xiii] G.W. Anderson, M.C. Hanf, P.R. Norton, Z.H. Lu, M.J. Graham *Appl. Phys. Lett.* 66 (1995) 1123-25.
- [xiv] D. Bodlaki, H. Yamamoto, D.H. Waldeck, E. Borguet, *Surf. Sci.* 543 (2003) 63-74.
- [xv] C. Fleischmann, S. Sioncke, S. Couet, K. Schouteden, B. Beckhoff, M. Müller, P. Hönicke, M. Kolbe, C. Van Haesendonck, M. Meuris, K. Temst, A. Vantomme, *J. Electrochem. Soc.*, 158 (2011) H589-H594.

- [xvi] C. Fleischmann, K. Schouteden, M. Müller, P. Hönicke, B. Beckhoff, S. Sioncke, H.G. Boyen, M. Meuris, C. VanHaesendonck, K. Temst, A. Vantomme, *Mater. Chem. C*, 1 (2013) 4105.
- [xvii] P.W. Loscutoff and S.F. Bent, *Annu. Rev. Phys. Chem.* 57 (2006) 467–495.
- [xviii] K. Choi and J.M. Buriak, *Langmuir*, 16 (2000) 7737-7741.
- [xix] T. Deegan, G. Hughes, *Appl. Surf. Sci.* 123/124 (1998) 66-70.
- [xx] S. Rivillon, Y.J. Chabal, F. Amy, A. Kahn, *Appl. Phys. Lett.* 87 (2005) 253101.
- [xxi] N. Cerniglia and P. Wang, *J. Electrochem. Soc.* 109 (1962) 508-512.
- [xxii] C. Mui, J. P. Senosiain, C. B. Musgrave, *Langmuir* 20 (2004) 7604-7609.
- [xxiii] K. Park, Y. Lee, J. Lee, S. Lim, *Applied Surface Science* 254 (2008) 4828–4832.
- [xxiv] Y. Lee, K. Park, S. Lim, *Appl. Surf. Sci.* 255 (2008) 3318–3321.
- [xxv] B. Schwartz, H. Robbins, *J. Electrochem. Soc.* 111 (1964) 196-201.
- [xxvi] B. Schwartz, *J. Electrochem. Soc.* 114 (1967) 285-291.
- [xxvii] S. Carturan, D. De Salvador, O. Lytovchenko, A. Mazzolari, G. Maggioni, M. Giarola, G. Mariotto, A. Carnera, G. Della Mea, V. Guidi, *Mat. Chem. Phys.* 132 (2012) 641– 651.
- [xxviii] S.-S. Bae, D.H. Kim, A. Kim, S. J. Jung, S. Hong, S. Kim, *J. Phys. Chem. C* 111 (2007) 15013-15019.
- [xxix] W.W. Harvey, H.C. Gatos, *J. Electrochem. Soc.* 107 (1960) 65-72.
- [xxx] M. Steinert, J. Acker, S. Oswald, K. Wetzig, *J. Phys. Chem. C* 111 (2007) 2133-2140.
- [xxxi] K. Prabhakaran, T. Ogino, *Surf. Sci.* 325 (1995) 263-271.
- [xxxii] T. Maeda, S. Takagi, T. Ohnishi and M. Lippmaa, *Mater. Sci. Semicond. Process.* 9 (2006) 706–710.
- [xxxiii] H. Seo, K.B. Chung, J.P. Long, G. Lucovsky, *J. Electrochem. Soc.* 156 (2009) H813-H817.
- [xxxiv] G. Maggioni, M. Gelain, D.R. Napoli, S. Carturan, J. Eberth, manuscript in preparation.